




RESEARCH ARTICLE | FEBRUARY 02 2026

## Revisiting the electron affinity of selenium

Rui Zhang ; Wenru Jie ; Jiayi Chen; Qihan Liu; Chuangang Ning  



*J. Chem. Phys.* 164, 054303 (2026)

<https://doi.org/10.1063/5.0311920>



### Articles You May Be Interested In

Rotational envelope simulations in photodetachment spectroscopy: Precise measurement of electron affinity of NO and O<sub>2</sub>

*J. Chem. Phys.* (July 2025)

Low-lying vibronic level structure of the ground state of the methoxy radical: Slow electron velocity-map imaging (SEVI) spectra and Köppel-Domcke-Cederbaum (KDC) vibronic Hamiltonian calculations

*J. Chem. Phys.* (June 2017)

High-resolution photoelectron imaging spectroscopy of cryogenically cooled Fe<sub>4</sub>O<sup>-</sup> and Fe<sub>5</sub>O<sup>-</sup>

*J. Chem. Phys.* (August 2016)

## AIP Advances

### Why Publish With Us?



**21DAYS**  
average time  
to 1st decision



**OVER 4 MILLION**  
views in the last year



**INCLUSIVE**  
scope

[Learn More](#)

# Revisiting the electron affinity of selenium

Cite as: J. Chem. Phys. 164, 054303 (2026); doi: 10.1063/5.0311920

Submitted: 12 November 2025 • Accepted: 9 January 2026 •

Published Online: 2 February 2026



View Online



Export Citation



CrossMark

Rui Zhang,  Wenru Jie,  Jiayi Chen, Qihan Liu, and Chuangang Ning<sup>a)</sup> 

## AFFILIATIONS

Department of Physics, State Key Laboratory of Low Dimensional Quantum Physics, Frontier Science Center for Quantum Information, Tsinghua University, Beijing 100084, China

<sup>a)</sup> Author to whom correspondence should be addressed: [ningcg@tsinghua.edu.cn](mailto:ningcg@tsinghua.edu.cn)

## ABSTRACT

The electron affinity (EA) of atomic selenium, previously established as  $16\,297.276(9)\text{ cm}^{-1}$  based on the laser photodetachment microscopy (LPM) measurements in 2012, exhibited a significant deviation from other earlier experimental values, yet it remained the accepted reference standard for over a decade. In this letter, we re-examined the EA of Se using the slow-electron velocity-map imaging method and revealed a substantial deviation in the LPM result. Measurements for the different isotopes of Se and the energy-level splitting of the neutral Se atom's  $^3P_2\text{--}^3P_1$  further verified the accuracy and robustness of our SEVI method. Based on this experimental evidence, we recommended a revised EA(Se) value of  $16\,297.78(4)\text{ cm}^{-1}$ , which is in excellent agreement with the previous laser photodetachment threshold experimental results.

Published under an exclusive license by AIP Publishing. <https://doi.org/10.1063/5.0311920>

## I. INTRODUCTION

Electron affinity (EA), defined as the energy difference between a neutral species and its corresponding anion in their respective ground states, is a fundamental parameter for understanding the behavior of atoms and molecules in diverse chemical and physical phenomena.<sup>1–3</sup> The precise measurement of EAs for elements in the periodic table remains an active research frontier in experimental physics and chemistry.<sup>4–8</sup> Notably, the most accurate EA measurement to date is for the main group element oxygen (O): the laser photodetachment threshold (LPT) method yielded an EA value of  $1.461\,112\,972(87)\text{ eV}$ , or  $11\,784.6709(8)\text{ cm}^{-1}$ .<sup>9</sup>

Selenium (Se, atomic number  $Z = 34$ ), a heavier group congener of oxygen, has an experimentally controversial EA value. The electron affinity of selenium was first measured as  $16\,297(2)\text{ cm}^{-1}$  using the LPT method by Hotop *et al.*<sup>10</sup> in 1973. They also simultaneously determined the spin-orbit splitting between  $^2P_{3/2}$  and  $^2P_{1/2}$  states of the  $\text{Se}^-$  anion to be  $2279(2)\text{ cm}^{-1}$ . Subsequent measurements by Mansour *et al.*<sup>11</sup> in 1988 achieved a tenfold improvement in precision, reporting  $\text{EA}(\text{Se}) = 16\,297.8(2)\text{ cm}^{-1}$  through tunable dye laser photodetachment spectroscopy combined with a Penning ion trap. Another independent LPT measurement by Thøgersen *et al.*<sup>12</sup> confirmed this EA value with a comparable precision [ $16\,297.7(4)\text{ cm}^{-1}$ ], while refining the spin-orbital splitting  $^2P_{3/2}\text{--}^2P_{1/2}$  to  $2278.2(2)\text{ cm}^{-1}$  in both single-photon and multiphoton absorption regimes. A notable discrepancy emerged when Vandevraye *et al.*<sup>13</sup> reported a significantly higher-precision EA(Se)

value of  $16\,297.276(9)\text{ cm}^{-1}$  employing the laser photodetachment microscope (LPM) method, which deviates significantly from the previous LPT results. However, Vandevraye *et al.* claimed that investigating the reasons for a possible overestimation of the detachment thresholds method was beyond the scope of their study, and they maintained their conclusion.

Despite the ongoing debate surrounding the electron affinity of selenium, the LPM measurement result has still remained the primary reference standard for over a decade. This persistent controversy of EA(Se) has motivated our re-examination of EA(Se) using slow-electron velocity-map imaging (SEVI) spectroscopy.<sup>14,15</sup> The SEVI method has demonstrated its robustness in many EA measurements thanks to its high energy resolution and ability to resolve multiple photodetachment channels. The SEVI technique has been successfully employed to accurately determine the EAs of the main group elements such as O, S, As, Sb, and Pb,<sup>8,16–18</sup> achieving accuracies typically better than  $0.1\text{ cm}^{-1}$ . In addition, this method has also been successfully applied to determine EAs across numerous transitional elements, lanthanides, and actinides, with typical accuracies of  $0.01\text{--}0.1\text{ meV}$ .<sup>7,8,19–21</sup> Given these proven capabilities, we present a reinvestigation of selenium's electronic structure and its anion, trying to solve the discrepancy using the SEVI spectroscopy.

## II. EXPERIMENTAL METHODS

The experiment was conducted on our Cryo-SEVI apparatus, as detailed elsewhere.<sup>22–24</sup> In this study,  $\text{Se}^-$  anions were generated

via laser ablation of a molten selenium target with helium carrier gas delivered through a pulsed valve under a backing pressure of around  $3 \times 10^5$  Pa. The produced anions were then accumulated in a radio frequency (RF) octupole ion trap,<sup>25</sup> assisted by a RF hexapole guide. The trapped anions lost their kinetic energies through continuous collisions with the buffer gas helium for  $\sim 45$  ms. Subsequently, the anions were extracted from the ion trap and mass-selected via a time-of-flight spectrometer.<sup>26</sup> The selected  $\text{Se}^-$  anions were then photodetached by a linearly polarized dye laser (Spectra-Physics) in the photodetachment region, with the wavelength monitored by a wavelength meter (HighFinesse WS6-600) with an accuracy of  $0.02 \text{ cm}^{-1}$ . The detached photoelectrons were analyzed via a velocity-map imaging (VMI) spectrometer,<sup>27,28</sup> and the imaging voltage was set as 75 V for the EA measurement. The distribution of outgoing photoelectrons can be reconstructed from the projected image using the maximum entropy velocity Legendre reconstruction (MEVELER) method<sup>29</sup> because the photoelectron distribution has a cylindrical symmetry. The kinetic energy of the photoelectrons was given by  $E_k = \alpha r^2$ , where  $r$  is the weighted center radius of the reconstructed three-dimensional spherical shell and  $\alpha$  is the calibration coefficient. The center position of the peak ( $r$ ) was determined via Gaussian function fitting. The binding energy (BE) of each transition was calculated using Einstein's equation,  $\text{BE} = h\nu - E_k$ , where  $h\nu$  is the photon energy of the detachment laser. The SEVI setup runs at a repetition rate of 20 Hz. Each photoelectron spectrum was acquired by accumulating 50 000 laser shots typically.

### III. RESULTS AND DISCUSSION

#### A. High-resolution photoelectron spectra of $\text{Se}^-$

Figure 1 shows the photoelectron spectra of  $\text{Se}^-$  anions acquired at two different photodetachment wavelengths using a tunable dye laser. The spectra exhibit no observable contamination from hydride species  $\text{SeH}^-$ , despite Se having several natural isotopes ( $m = 74, 76, 77, 78, 80, 82$ ). This spectral purity is attributable to the significant EA difference between  $\text{SeH}^-$  [2.21(3) eV] and  $\text{Se}^-$  [2.020 67(2) eV], enabling complete spectral discrimination.<sup>30</sup> Figure 1(b) presents the corresponding schematic energy-level diagram of anionic and neutral Se states. Three transitions from anionic  $\text{Se}^-$  to neutral Se (labeled A–C) were observed in the photoelectron spectra. Peak A is the photodetachment transition from the anionic ground state  $\text{Se}^- (^2P_{3/2})$  to the neutral ground state  $\text{Se} (^3P_2)$ . Its binding energy was preliminarily determined to be  $16\,297.78(64) \text{ cm}^{-1}$ , directly representing the electron affinity of atomic selenium. More precise measurements of this EA value will be detailed in Subsection III B. Peak B is the transition from the anionic ground state  $\text{Se}^- (^2P_{3/2})$  to the neutral first excited state  $\text{Se} (^3P_1)$ , and its binding energy was determined as  $18\,287.26(83) \text{ cm}^{-1}$ . Peak C is the transition from the first excited state of  $\text{Se}^- (^2P_{1/2})$  to the first excited state of  $\text{Se} (^3P_1)$ , with a binding energy determined as  $16\,011(1) \text{ cm}^{-1}$ . The weak intensity of peak C reflects the low population of the anionic excited state  $^2P_{1/2}$ . It remains detectable thanks to the high energy resolution and high sensitivity of our SEVI spectrometer. By subtracting the binding energies of transitions B and C, the spin-orbital splitting of  $^2P_{1/2} - ^2P_{3/2}$  of the negative ion was determined to be  $2276(2) \text{ cm}^{-1}$ , which is consistent with the previously reported high-precision value of  $2278.2(2) \text{ cm}^{-1}$ .<sup>12</sup> The peak widths of peaks A and B, fitted with Gaussian functions, demonstrate our instrument's

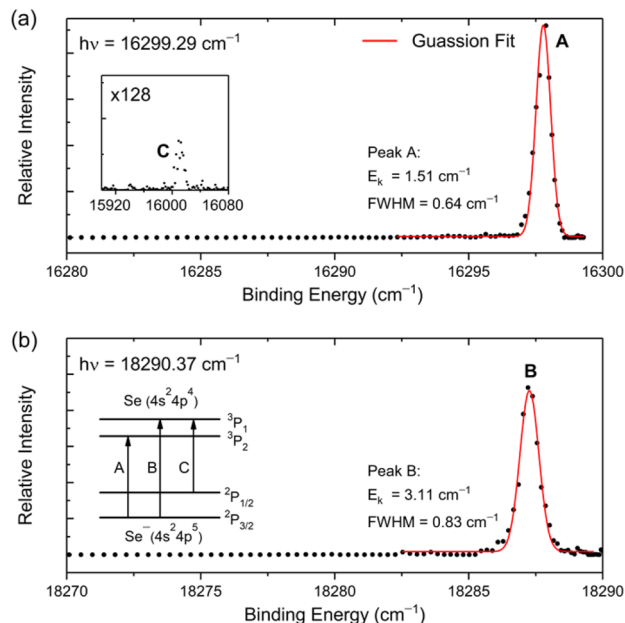
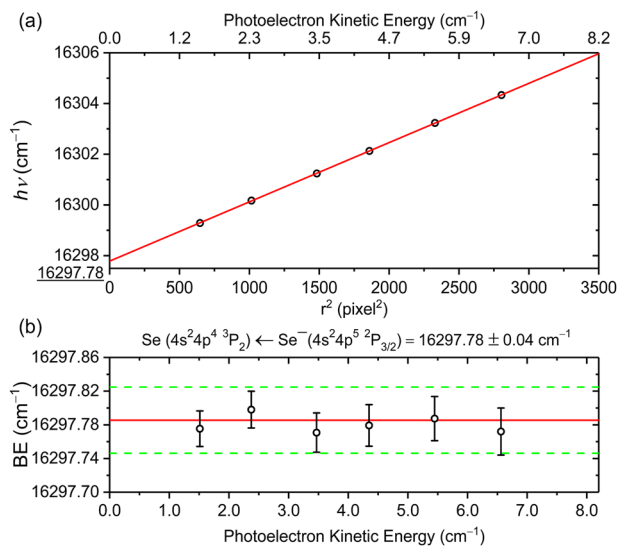


FIG. 1. Photoelectron spectra of  $\text{Se}^-$  obtained at photon energies (a)  $16\,299.29 \text{ cm}^{-1}$  and (b)  $18\,290.37 \text{ cm}^{-1}$ . The inset in (a) shows the magnified view of peak C, and the inset in (b) shows the assignment of peaks A–C. The kinetic energies ( $E_k$ ) and FWHMs for peaks A and B are also labeled.

resolution: the full width at half maximum (FWHM) of peak A is  $0.64 \text{ cm}^{-1}$  with kinetic energy  $E_k = 1.51 \text{ cm}^{-1}$ . Similarly, the FWHM of peak B is  $0.83 \text{ cm}^{-1}$  with  $E_k = 3.11 \text{ cm}^{-1}$ . The energy resolution of our SEVI apparatus is comparable with the values reported by the Wang group (FWHM =  $1.2 \text{ cm}^{-1}$  at  $E_k = 5.2 \text{ cm}^{-1}$ )<sup>28</sup> and by the Neumark group (FWHM =  $1.1 \text{ cm}^{-1}$  at  $E_k = 1.8 \text{ cm}^{-1}$ ).<sup>31</sup>

#### B. Precise measurement of the electron affinity of Se

To accurately determine the electron affinity of Se, the photon energy  $h\nu$  of the detachment laser was carefully tuned slightly above the photodetachment threshold of transition A. Sequential spectra spanning from  $16\,299$  to  $16\,305 \text{ cm}^{-1}$  were acquired at  $1 \text{ cm}^{-1}$  intervals. Since the kinetic energy of photoelectrons is proportional to the squared radius ( $r^2$ ) of the photoelectron sphere, a linear regression analysis on the  $h\nu$  vs  $r^2$  was implemented in Fig. 2 based on Einstein's photoelectric equation  $h\nu = \text{BE} + \alpha r^2$ . The binding energy of the transition  $\text{Se} (^3P_2) \leftarrow \text{Se}^- (^2P_{3/2})$  was given by the vertical-axis intercept. This analysis yielded a refined EA(Se) value of  $16\,297.78 \pm 0.04 \text{ cm}^{-1}$ , equivalent to  $2.020\,667(5) \text{ eV}$  using the 2018 CODATA conversion ( $1 \text{ eV} = 8065.543\,937 \dots \text{ cm}^{-1}$ ).<sup>32</sup> The total uncertainty of  $0.04 \text{ cm}^{-1}$  includes a systematic uncertainty of  $0.02 \text{ cm}^{-1}$  from the wavelength meter. To evaluate the isotope effects on the EA measurement for the Se atom, we measured the binding energies of transition A for five primary isotopes of selenium:  $^{76}\text{Se}$  (abundance 9%),  $^{77}\text{Se}$  (8%),  $^{78}\text{Se}$  (24%),  $^{80}\text{Se}$  (50%), and  $^{82}\text{Se}$  (9%). Our measurement suggested that the isotope shifts remain below  $0.03 \text{ cm}^{-1}$ , within experimental uncertainty. In addition, we also changed the imaging voltage from 75 to 150 V. No observable difference was detected between the two imaging voltages. This



**FIG. 2.** (a) Photon energy ( $h\nu$ ) vs squared radius ( $r^2$ ) of photoelectron spherical shells for the transition A. The red solid line represents a linear least-squares fit, where the intercept,  $16\,297.78\text{ cm}^{-1}$ , is the measured EA value of selenium. (b) The binding energy (BE) of transition A as a function of the photoelectron kinetic energy. The green dashed lines represent  $\pm 0.04\text{ cm}^{-1}$  uncertainty.

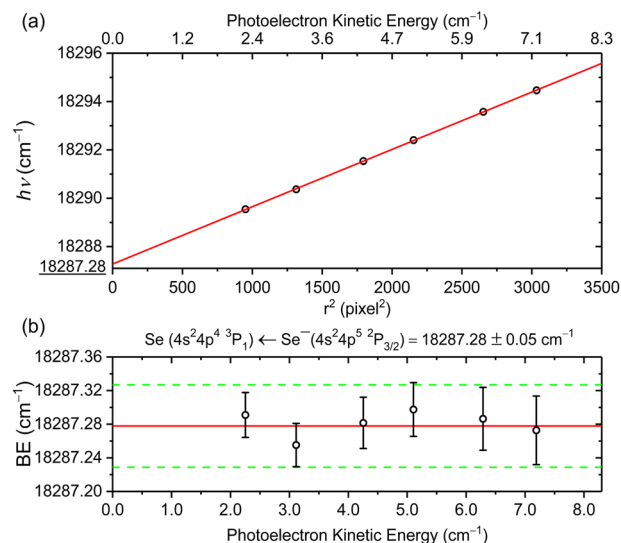


**FIG. 3.** (a) Photon energy ( $h\nu$ ) vs squared radius ( $r^2$ ) of photoelectron spherical shells for the transition B. The binding energy of transition B is determined to be  $18\,287.28\text{ cm}^{-1}$  via a linear least-squares fit. (b) The binding energy (BE) of transition B as a function of the photoelectron kinetic energy. The green dashed lines represent  $\pm 0.05\text{ cm}^{-1}$  uncertainty.

**TABLE I.** Measured EA(Se) values for various isotopes of Se with two imaging voltages.

| Isotope          | Imaging voltage (V) | EA(Se) ( $\text{cm}^{-1}$ ) |
|------------------|---------------------|-----------------------------|
| $^{76}\text{Se}$ | 150                 | $16\,297.77(6)$             |
| $^{76}\text{Se}$ | 75                  | $16\,297.78(4)$             |
| $^{77}\text{Se}$ | 75                  | $16\,297.76(4)$             |
| $^{78}\text{Se}$ | 75                  | $16\,297.78(4)$             |
| $^{80}\text{Se}$ | 75                  | $16\,297.79(4)$             |
| $^{82}\text{Se}$ | 75                  | $16\,297.79(4)$             |

result further excludes so-called “quantum offset” effects<sup>18,33</sup> in the SEVI experiments, which incorrectly claimed that SEVI results have field-dependent systematic deviations of  $0.185\text{ cm}^{-1}$  at 75 V and  $0.292\text{ cm}^{-1}$  at 150 V.<sup>33</sup> Table I lists the measured EA(Se) values for various selenium isotopes and the corresponding imaging voltages.

### C. Verification via an alternative transition

To verify the reliability of our EA(Se) measurement, we also accurately measured the binding energy of transition B  $^2P_{3/2}(\text{Se}^-) \rightarrow ^3P_1(\text{Se})$  using the same method. Since transitions A and B are both from the same anionic ground state, the energy difference between these two transitions equals the spin-orbital splitting of the final states  $\text{Se}(^3P_2)$  and  $\text{Se}(^3P_1)$ , which is well known to be  $1989.497\text{ cm}^{-1}$  according to the NIST atomic data.<sup>34,35</sup> As shown in Fig. 3, the squared radius  $r^2$  was plotted vs the photon energy  $h\nu$  ranging from 18 289 to 18 294  $\text{cm}^{-1}$ . The binding energy of the transition  $\text{Se}(^3P_1) \leftarrow \text{Se}^-(^2P_{3/2})$  was determined to be  $18\,287.28(5)\text{ cm}^{-1}$ . The  $^3P_2\text{--}^3P_1$  energy-level splitting of Se was obtained by

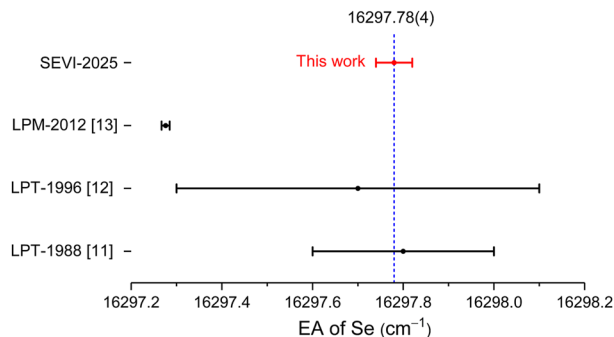
subtracting the binding energies of transition A from that of B, yielding a value of  $1989.50(7)\text{ cm}^{-1}$ . This splitting value is in excellent agreement with the NIST reference result of  $1989.497\text{ cm}^{-1}$ , which further confirms the reliability of our experimental results of EA(Se). In other words, this alternative channel also yielded EA(Se) =  $16\,297.78(5)\text{ cm}^{-1}$  by subtracting the reference splitting  $1989.497\text{ cm}^{-1}$  from the binding energy  $18\,287.28(5)\text{ cm}^{-1}$ , which is in excellent agreement with the value  $16\,297.78(4)\text{ cm}^{-1}$  obtained via the transition  $\text{Se}(^3P_2) \leftarrow \text{Se}^-(^2P_{3/2})$ . All measured binding energies of transitions A–C are recorded in Table II.

Figure 4 compares experimental EA values of Se with the previously reported results. For clarity, the early LPT result, EA(Se) =  $16\,297(2)\text{ cm}^{-1}$  by Hotop *et al.* in 1973, is omitted due to their substantially large error bar, making the other small error bar invisible when plotted on the same scale.<sup>10</sup> Our SEVI measurement result is consistent with the values of Thøgersen *et al.*<sup>12</sup> and Mansour *et al.*<sup>11</sup> using the LPT method. The accuracy of our SEVI result represents an improvement of an order of magnitude over previous LPT measurements. A striking discrepancy emerges when comparing with the previously accepted benchmark LPM EA(Se) =  $16\,297.276(9)\text{ cm}^{-1}$  reported by Vandevrage *et al.*<sup>13</sup> Their reported value

**TABLE II.** Binding energies of observed transitions A–C.

| Peak | Transition ( $\text{Se}^- \rightarrow \text{Se}$ ) <sup>a</sup> | Binding energy ( $\text{cm}^{-1}$ ) |
|------|---|-------------------------------------|
| A    | $^2P_{3/2} \rightarrow ^3P_2$                                   | $16\,297.78(4)$                     |
| B    | $^2P_{3/2} \rightarrow ^3P_1$                                   | $18\,287.28(5)$                     |
| C    | $^2P_{1/2} \rightarrow ^3P_1$                                   | $16\,011(1)$                        |

<sup>a</sup>The electronic configuration of  $\text{Se}^-$  is  $4s^24p^5$ , while that of Se is  $4s^24p^4$ .



**FIG. 4.** Comparison of experimental EA(Se) values with error bars reported by different groups. The blue dashed line represents a recommendation EA(Se) value weighted by the SEVI and LPT measurements.

deviates by  $0.50\text{ cm}^{-1}$  from the consensus—50 times greater than their claimed uncertainty, indicating LPM alone cannot benchmark other methods.

Based on the above-mentioned evidence, we can safely conclude that there is a significant deviation in the previous LPM result. Actually, Vandevrage *et al.*<sup>13</sup> pointed out that their experimental methodology employed for EA measurements exhibited systematic energy shifts correlated with the electric field in the photodetachment region. This estimated electric-field uncertainty reached  $\sim 2.5\%$  in their LPM measurements of EA(Se), while their earlier EA measurements on phosphorus (P) demonstrated a markedly lower field-induced error of  $-0.3\%$ .<sup>36</sup> Vandevrage *et al.*<sup>13</sup> acknowledged that this discrepancy between these two systematic errors observed in LPM measurements remained a mystery.

#### IV. CONCLUSIONS

In summary, we have revisited the electron affinity of selenium with the SEVI method and pointed out a significant deviation from the previously reported LPM result of EA(Se). Based on our new SEVI results and earlier LPT measurements, we updated the recommended value of EA(Se) as  $16297.78(4)\text{ cm}^{-1}$ , resolving the longstanding discrepancies among prior EA(Se) measurements.

#### ACKNOWLEDGMENTS

This study was supported by the National Natural Science Foundation of China (NSFC) (Grant Nos. 12374244 and 12341401).

#### AUTHOR DECLARATIONS

##### Conflict of Interest

The authors have no conflicts to disclose.

##### Author Contributions

**Rui Zhang:** Investigation (lead); Writing – original draft (lead); Writing – review & editing (supporting). **Wenru Jie:** Investigation (supporting). **Jiayi Chen:** Investigation (supporting). **Qihan Liu:** Investigation (supporting). **Chuangang Ning:** Funding acquisition (lead); Investigation (lead); Writing – original draft (supporting); Writing – review & editing (lead).

#### DATA AVAILABILITY

The data that support the findings of this study are available from the corresponding author upon reasonable request.

#### REFERENCES

- 1 T. Andersen, *Phys. Rep.* **394**, 157–313 (2004).
- 2 W. C. Lineberger, *Annu. Rev. Phys. Chem.* **64**, 21–36 (2013).
- 3 J. C. Rienstra-Kiracofe, G. S. Tschumper, H. F. Schaefer, S. Nandi, and G. B. Ellison, *Chem. Rev.* **102**, 231–282 (2002).
- 4 H. Hotop and W. C. Lineberger, *J. Phys. Chem. Ref. Data* **4**, 539–576 (1975).
- 5 H. Hotop and W. C. Lineberger, *J. Phys. Chem. Ref. Data* **14**, 731–750 (1985).
- 6 T. Andersen, H. K. Haugen, and H. Hotop, *J. Phys. Chem. Ref. Data* **28**, 1511–1533 (1999).
- 7 C. Ning and Y. Lu, *J. Phys. Chem. Ref. Data* **51**, 021502 (2022).
- 8 S. Yan, Y. Lu, R. Zhang, and C. Ning, *Chin. J. Chem. Phys.* **37**, 1–12 (2024).
- 9 M. K. Kristiansson, K. Chartkunchand, G. Eklund, O. M. Hole, E. K. Anderson, N. de Ruette, M. Kamińska, N. Punnakayathil, J. E. Navarro-Navarrete, S. Sigurdsson, J. Grumer, A. Simonsson, M. Björkhage, S. Rosén, P. Reinhed, M. Blom, A. Källberg, J. D. Alexander, H. Cederquist, H. Zettergren, H. T. Schmidt, and D. Hanstorp, *Nat. Commun.* **13**, 5906 (2022).
- 10 H. Hotop, T. A. Patterson, and W. C. Lineberger, *Phys. Rev. A* **8**, 762–774 (1973).
- 11 N. B. Mansour, C. J. Edge, and D. J. Larson, *Nucl. Instrum. Methods Phys. Res., Sect. B* **31**, 313–316 (1988).
- 12 J. Thøgersen, L. D. Steele, M. Scheer, H. K. Haugen, P. Kristensen, P. Balling, H. Stapelfeldt, and T. Andersen, *Phys. Rev. A* **53**, 3023–3028 (1996).
- 13 M. Vandevrage, C. Drag, and C. Blondel, *Phys. Rev. A* **85**, 015401 (2012).
- 14 C. Hock, J. B. Kim, M. L. Weichman, T. I. Yacovitch, and D. M. Neumark, *J. Chem. Phys.* **137**, 244201 (2012).
- 15 R. Tang, X. Fu, and C. Ning, *J. Chem. Phys.* **149**, 134304 (2018).
- 16 R. Tang, X. Fu, Y. Lu, and C. Ning, *J. Chem. Phys.* **152**, 114303 (2020).
- 17 C. X. Song, S. T. Yan, M. Godefroid, J. Bierón, P. Jönsson, G. Gaigalas, J. Ekman, X. M. Zhang, C. Y. Chen, C. G. Ning, and R. Si, *J. Chem. Phys.* **160**, 214307 (2024).
- 18 R. Zhang, S. Yan, W. Jie, J. Chen, Q. Liu, and C. Ning, *arXiv:2510.17204* (2025).
- 19 Z. Luo, X. Chen, J. Li, and C. Ning, *Phys. Rev. A* **93**, 020501 (2016).
- 20 Y. Lu, R. Tang, X. Fu, and C. Ning, *Phys. Rev. A* **99**, 062507 (2019).
- 21 R. Tang, R. Si, Z. Fei, X. Fu, Y. Lu, T. Brage, H. Liu, C. Chen, and C. Ning, *Phys. Rev. Lett.* **123**, 203002 (2019).
- 22 R. Zhang, Y. Lu, R. Tang, and C. Ning, *J. Chem. Phys.* **158**, 084303 (2023).
- 23 Y. Lu, R. Zhang, C. Song, C. Chen, R. Si, and C. Ning, *Chin. Phys. Lett.* **40**, 093101 (2023).
- 24 R. Zhang, Y. Lu, S. Yan, and C. Ning, *Phys. Rev. A* **111**, 023102 (2025).
- 25 J. B. Kim, M. L. Weichman, and D. M. Neumark, *Mol. Phys.* **113**, 2105–2114 (2015).
- 26 W. C. Wiley and I. H. McLaren, *Rev. Sci. Instrum.* **26**, 1150–1157 (2004).
- 27 A. T. J. B. Eppink and D. H. Parker, *Rev. Sci. Instrum.* **68**, 3477–3484 (1997).
- 28 I. León, Z. Yang, H.-T. Liu, and L.-S. Wang, *Rev. Sci. Instrum.* **85**, 083106 (2014).
- 29 B. Dick, *Phys. Chem. Chem. Phys.* **16**, 570–580 (2014).
- 30 K. C. Smyth and J. I. Brauman, *J. Chem. Phys.* **56**, 5993–5997 (1972).
- 31 A. Osterwalder, M. J. Nee, J. Zhou, and D. M. Neumark, *J. Chem. Phys.* **121**, 6317–6322 (2004).
- 32 E. Tiesinga, P. J. Mohr, D. B. Newell, and B. N. Taylor, *Rev. Mod. Phys.* **93**, 025010 (2021).
- 33 C. Blondel and C. Drag, *Phys. Rev. Lett.* **134**, 043001 (2025).
- 34 K. B. S. Eriksson, *Phys. Lett.* **41**, 97–98 (1972).
- 35 J. E. Sansonetti and W. C. Martin, *J. Phys. Chem. Ref. Data* **34**, 1559–2259 (2005).
- 36 R. J. Peláez, C. Blondel, M. Vandevrage, C. Drag, and C. Delsart, *J. Phys. B: At., Mol. Opt. Phys.* **44**, 195009 (2011).